Astrophys Space Sci (2009) 322: 101–105
DOI 10.1007/s10509-008-9897-1

ORIGINAL ARTICLE

Laboratory experiments to study supersonic astrophysical flows interacting with clumpy environments

P.A. Rosen · J.M. Foster · B.H. Wilde · P. Hartigan · B.E. Blue · J.F. Hansen · C. Sorce · R.J.R. Williams · R. Coker · A. Frank

Received: 12 June 2008 / Accepted: 27 August 2008 / Published online: 20 September 2008

Abstract A wide variety of objects in the universe drive supersonic outflows through the interstellar medium which is often highly clumpy. These inhomogeneities affect the morphology of the shocks that are generated. The hydrodynamics are difficult to model as the problem is inherently 3D and the clumps are subject to a variety of fluid instabilities as they are accelerated and destroyed by the shock. Over the last two years, we have been carrying out experiments at the University of Rochester's Omega laser to address the interaction of a dense-plasma jet with a localised density perturbation. More recently, we have turned our attention to the interaction of a shock wave with a spherical particle. We use a 1.6-mm diameter, 1.2-mm length Omega hohlraum to drive a composite plastic ablator (which includes bromine to prevent M-band radiation from preheating the experiment). The ablator acts as a "piston" driving a shock into 0.3 $\mathrm{g\,cm^{-3}}$ foam containing a 0.5-mm diameter sapphire sphere. We radiograph along two orthogonal lines of sight, using nickel or zinc pinhole-apertured X-ray backlighters, to study the subsequent hydrodynamics. We present initial experimental results and two-dimensional simulations of the experiment.

Keywords Laboratory astrophysics · Supersonic astrophysical flows · Shocked clumps · Omega laser

P.A. Rosen (✉) · J.M. Foster · R.J.R. Williams
AWE Aldermaston, Reading, RG7 4PR, UK
e-mail: paula.rosen@awe.co.uk

B.H. Wilde · R. Coker
Los Alamos National Laboratory, Los Alamos, NM 87545, USA

P. Hartigan
Rice University, P.O. Box 1892, Houston, TX 77251-1892, USA

B.E. Blue
General Atomics, P.O. Box 85608, San Diego, CA 92186-5608, USA

J.F. Hansen · C. Sorce
Lawrence Livermore National Laboratory, Livermore, CA 94550, USA

A. Frank
University of Rochester, Rochester, NY 14627-0171, USA

1 Introduction

Much of the analysis of astrophysical flows relies upon models that make simplistic assumptions about the geometries of the flows. One of the most important of these assumptions, and one that is rarely realised in nature, is that of a pre-shock medium of uniform density. In real astrophysical situations, shock waves move into media that are often highly clumpy, which affects the morphology and spectra of material heated in the shocks, and also affects how the shocks propagate. It is difficult to model shocks that move into clumpy media in astrophysical situations because the problem is inherently 3D, and the clumps are subject to a variety of fluid instabilities as they are accelerated and destroyed by the shock (Poludnenko et al. 2002, 2004). Examples of shocked clumps in jets from young stars are shown in Fig. 1.

One way to shed some light on how shocks propagate into clumpy media is to recreate the situation in a laboratory plasma. In our previous NLUF-sponsored experiments (Foster et al. 2005 and Coker et al. 2007) at the Omega laser facility, we developed a well-characterised experimental 'test-bed' to study high-Mach-number, compressible, potentially turbulent, dense-plasma jets and their associated bow shocks, as they propagate through fluids that are either

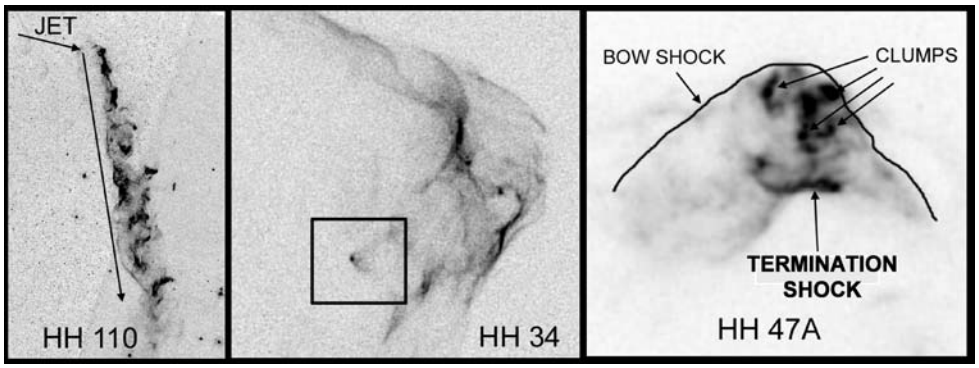

Fig. 1 Shocked clumps in jets from young stars. *Left* (**a**)—HST image of the HH 110 flow. The jet enters from the left, impacts a molecular cloud, and deflects downward, producing a spray of shocked gas. *Middle* (**b**)—HST images of the bow shock of protostellar jet HH 34. The large bow shock moves to the right in this image, and has overtaken a small clump shown in the box. *Right* (**c**)—An HST image of the HH 47A bow shock, showing a an inhomogeneous region. Images taken at a later time show that small clumps from the jet move upward through the Mach disk, and may survive all the way to the bow shock

homogeneous or contain a single, large-scale, density perturbation. These experiments were relevant to the astrophysical object HH110.

The new experiments, reported here, are addressing objects such as HH34 and HH47A, where small clumps become accelerated by much larger shocks. The experiment generates a strong, planar bow shock which collides with a spherical obstacle located at various distances from the axis of the flow.

In addition to the Omega experiments, astronomical observations have been carried out which measured velocity shear and turbulence in deflected and entrained flows. These used the telescope at Kitt Peak National Observatory (Hartigan et al. 2007a) and the Hubble Space telescope (Hartigan et al. 2007b).

Others have studied the interaction of a strong, near-planar shock with a single, spherical particle (Klein et al. 2000, 2003 and Robey et al. 2002). In the work by Klein and Robey, an ablative drive was used to launch a strong ($M = 10$) shock in a small (typically, 800 μm diameter) solid-polystyrene or foam-filled shock tube containing a single (typically, 100 μm diameter) spherical copper or aluminium particle. As in their experiments, we use X-ray backlighting radiography to record the hydrodynamic motion of this particle, in a succession of 'snapshot' images. These experiments are analogous to 'shock-bubble' experiments in conventional shock tubes (Haas and Sturtevant 1987; Jacobs 1993 and Ranjan et al. 2005), although significantly, the much higher Mach number available in the laser-driven case provides access to differences of hydrodynamic development for $M > 2$. In recent work (Hansen et al. 2007), the interaction of a strong shock with two adjacent aluminium spheres (120 μm diameter spheres in 0.3 $\mathrm{g\,cm^{-3}}$ density foam) has been studied.

Our present work builds on the experiments by Klein et al. Our longer-term goal is to study large shocks that overrun multiple small-diameter particles. That is, we will move from an experiment in which the jet/shock and density discontinuity scale sizes are comparable to one in which the scale sizes are significantly different (bow shock and planar shock propagation through small-scale clumpy medium).

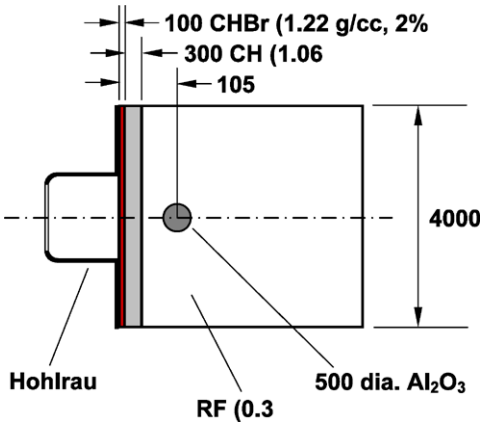

Fig. 2 The target design for the shock-sphere interaction experiment. All dimensions are in μm. The hohlraum measures 1.6 mm in diameter and is 1.2 mm long and the foam cylinder measure 4000 μm in length

2 Experiment configuration

The design for the experiments is shown in Fig. 2. Radiation drive is generated using a 1.6-mm-diameter, 1.2-mm-length cylindrical gold hohlraum target with a single 1.2-mm-diameter laser-entry hole. The experimental package is mounted over a 1.6-mm-diameter hole in the hohlraum, immediately opposite the laser entry hole. The hohlraum is heated by 12 beams of the Omega laser with a total energy of 6 kJ in a 1-ns duration, constant power laser pulse of 0.35-μm wavelength. The details and modelling

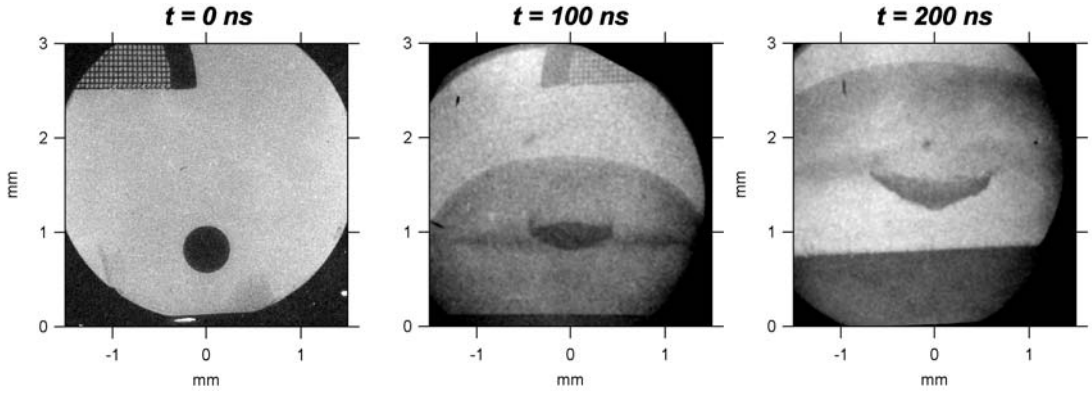

Fig. 3 Pre-shot radiograph ($t = 0$ ns) and experimental radiographs at $t = 100$ and 200 ns. The initial position (μm) of the ball (r, z) is (208, 1229), (160, 1114) and (166, 1195) respectively. The nominal position of the ball is (0, 1050) where $r = 0$ corresponds to a position on the cylindrically-symmetric axis of the experimental configuration and $z = 1050$ corresponds to the distance from the driven side of the ablator to the centre of the sapphire sphere. The radiographs are backlit with nickel

of this hohlraum are described in detail elsewhere (Foster et al. 2005). As the hohlraum used in the experiments described here has no end wall, the albedo is somewhat reduced and the resulting peak radiation temperature is lower (170–180 eV) than that in the previously referenced experiments. The hohlraum drives a composite plastic ablator consisting of a 100-μm thickness layer of CHBr (2% atomic Br, and 1.22 g cm^{-3} density) and a 300 μm thickness layer of CH (polystyrene of 1.06 g cm^{-3} density). The ablator acts as a 'piston' driving a shock into foam containing a 500-μm-diameter sapphire sphere. The foam comprises a 4-mm diameter, 6-mm length cylinder of resorcinol-formaldehyde ($C_{15}H_{12}O_4$) foam, of 0.3 g cm^{-3} density. Resorcinol-formaldehyde foam is used because of its very small (<1 μm) pore size. The centre of the sapphire sphere is placed 1050 μm from the driven surface of the ablator along the cylindrical axis of symmetry ($r = 0$). The precise position of the sapphire sphere is measured pre-shot, for each target, via dual-axis X-ray radiography. The precise position of the sphere inevitably varies from target to target. The size of the sapphire sphere is chosen such that the radius of curvature of the shock is much greater that the radius of curvature of the sphere (see Sect. 4 below).

The evolution of the shock-sphere interaction is diagnosed by X-ray backlighting radiography, using a pinhole-apertured, laser-produced-plasma, X-ray backlighting source to project an image of the sphere either directly onto radiographic film or via a gated micro-channel-plate detector onto film. Both nickel and zinc are (separately) used as backlighter materials. The He-like resonance lines of nickel and zinc are 7806 and 8999 eV respectively and lie above the K-absorption edge of aluminium (1560 eV). The backlighter foils are illuminated with three laser beams (∼425 J per beam) in a 1-ns duration laser pulse (0.35-μm wavelength).

Figure 3 shows experimental radiographs, backlit with nickel, from two separate laser shots, backlit at $t = 100$ and 200 ns together with a pre-shot radiograph (equivalent to $t = 0$ ns). The bow shock and distorted sphere are clearly visible in the latter two radiographs.

3 Modelling

The experiment is modelled using the RAGE (Gittings 1992) and PETRA (Youngs, 1982, 1984) hydrocodes. Due to limitation of space, only the AWE (PETRA) calculations will be described in this paper. The experimental geometry was calculated, but the physical presence of the hohlraum was not included in the calculation. Instead, the hohlraum drive was approximated by a Planckian temperature-time profile input in a region of low-density gold immediately adjacent to the ablator. The code uses tabular LTE opacities which are calculated off-line using the IMP (Rose 1992) opacity code. Equation-of-state data are also input in tabular form using the SESAME (Lyon and Johnson 1992) database. Square, 5 μm zones are used in the central part of the problem (up to a radius of 800 μm), then the size of the radial zones increases geometrically, with an increase in cell size of 10% per cell (to limit the overall number of cells in the problem to make the calculation run more efficiently). The simulation is post-processed to produce a synthetic radiograph for comparison with the experimental data.

4 Hydrodynamic scaling

In order for these experiments to be directly applicable to astrophysical objects, a number of hydrodynamic criteria must be met. In particular (Ryutov et al. 1999), in order to

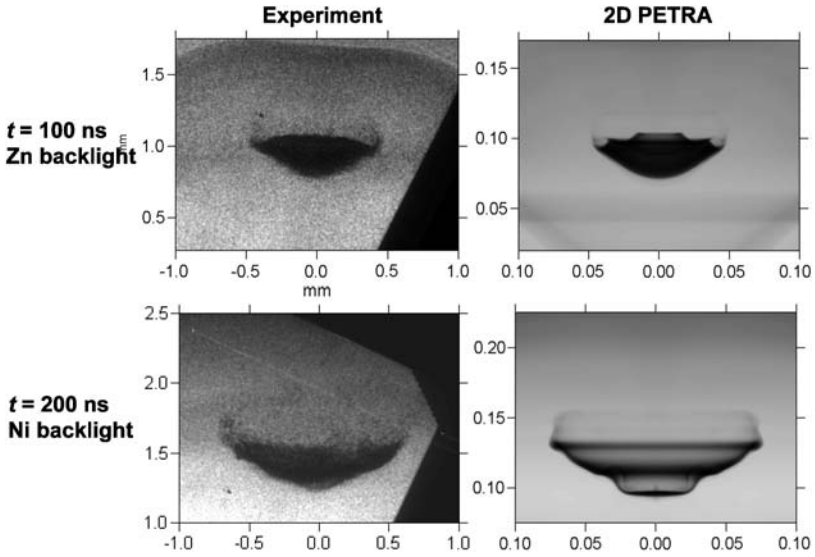

Fig. 4 Experimental radiographs and post-processed simulations at $t = 100$ and 200 ns, backlit with zinc and nickel respectively. The initial positions (μm) of the ball (r, z) in the experiment are (27, 1034) and (166, 1195) respectively. The position of the ball in the simulation is (0, 1050) where $r = 0$ corresponds to a position on the cylindrically-symmetric axis of the experimental configuration and $z = 1050$ corresponds to the distance from the driven side of the ablator to the centre of the sapphire sphere

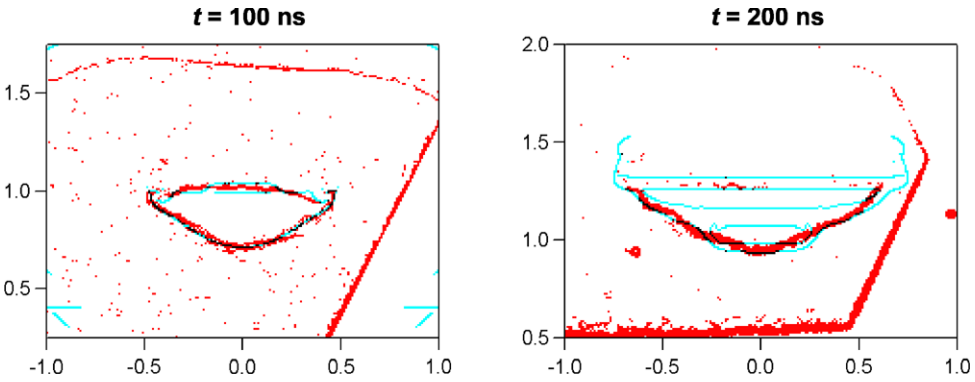

Fig. 5 Quantitative comparison of experimental data with post-processed simulation at $t = 100$ and 200 ns using an edge detection algorithm. Red represents experimental data and blue represents the PETRA simulation. Black denotes where the experiment and simulation agree precisely

scale, various dimensionless quantities must be comparable and both the laboratory and astrophysical systems must satisfy a number of dissipation criteria, such as negligible heat conduction, viscosity and energy loss by radiation. In practice, it has been found (Klein et al. 1994) that the behaviour of a strong shock running into an obstacle converges for Mach numbers above ∼2.5; we obtain experimental internal isothermal Mach numbers of ∼5. Another dimensionless number that must be matched is the density ratio η, of the obstacle to the surrounding medium. At present, the experiments have $\eta \sim 10$ while the astrophysical objects (cold clumps embedded in a warmer medium) probably have wide ranges of η, from ∼3 to 100 or more.

There are three timescales in shock/obstacle problems: the time it takes for the shock to cross the obstacle (t_c), the time it takes to destroy the obstacle (t_d), and the evolution timescale of the shock itself (t_s). For $\eta \sim 10$ and treating the shock as a Sedov blast wave (Klein et al. 2003), we have $t_c \sim 2r_0/v_s$, $t_d \sim 3r_0/v_s$, and $t_s \sim 0.1r_s/v_s$, where r_0 is the radius of the obstacle, r_s is the radius of curvature of the shock, and v_s is the velocity of the shock. Thus, in order to be in the ideal 'small cloud' limit, we need the shock to have a radius of curvature $r_s \gg r_0$. Note this only applies to the part of the shock that interacts with the obstacle. If we do not meet this requirement, the shock evolves significantly in the time of the experiment, and the experiment would be more like a YSO jet interacting with ISM clumps (where the clumps are on the order of the size of the shock front) than a SN blast wave overrunning ejecta.

For the Ryutov Euler scaling to be valid, dissipative mechanisms must be unimportant. That is, the system must be collisional ($l_{coll} \ll r_0$), thermal conduction must be small (Pe $\gg 1$), radiative cooling should be small over the relevant timescale ($t_{cool} \gg t_d$), and viscous dissipation should be negligible (Re $\gg 1$). Using representative values of $n \sim 10^{23}$ cm^{-3}, $T \sim 1$ eV, $v \sim 10^6$ cm s^{-1}, $A \sim 10$ amu, and $Z \sim 3$, and solving the expressions in Ryutov et al. (1999), we find that $l_{coll}/r_0 \sim 10^{-6}$, Pe $\sim 10^7$, $t_d/t_{cool} \sim 10^{-4}$, and Re $\sim 10^5$. Thus, hydrodynamic scaling of these experiments to astrophysical objects should apply. It should be noted that we are not fully in the decoupled regime (regions of the experiment have $\Gamma \geq 1$).

5 Comparison of experimental data with simulation

Figure 4 shows a comparison of experimental data at 100 and 200 ns with a post-processed simulation. The gross hydrodynamic features are reproduced well by the simulation. The question arises of how to make a meaningful quantitative comparison between experiment and simulation. It was decided to use an edge detection algorithm (Canny 1986) to compare the experimental data to the simulation. Figure 5 shows a comparison at $t = 100$ and 200 ns.

6 Summary

We have carried out an astrophysically-relevant experiment to study the interaction of a shock with a spherical "clump". The simulations broadly agree with the gross features present in the experimental data, but differ in the finer-scale structure. Further experiments are planned which refine some of the experimental details (e.g. a lower-opacity ball to probe the structure within the sphere). These experiments lay the foundation for an experimental study into the interaction of a shock with multiple clumps.

Acknowledgements We would like to thank Peter Graham (AWE) for modifying his subroutine which calculates volume fractions in PETRA, and for shedding light on some of the idiosyncrasies of PETRA and the AWE supercomputer. We also extend our thanks to the teams at General Atomics for target manufacture and characterisation and the laser and operations staff at the Omega laser facility.

References

Canny, J.: IEEE Trans. Pattern Anal. Mach. Intell. **8**, 679 (1986)
Coker, R.F., et al.: Astrophys. Space Sci. **307**, 57–62 (2007)
Foster, J.M., et al.: Astrophys. J. Lett. **634**, L77 (2005)
Gittings, M.L.: Numerical Methods Symposium, April 28–30 (1992). Copies may be ordered from the Defence Nuclear Agency, 56801 Telegraph Road, Alexandria, VA 22310-3398
Haas, J.-F., Sturtevant, B.: J. Fluid Mech. **181**, 41 (1987)
Hansen, J.F., et al.: Astrophys. Space Sci. **307**, 147–152 (2007)
Hartigan, P., et al.: Proposal 06B-0182 (2007a)
Hartigan, P., et al.: Proposal 11179 (2007b)
Lyon, S.P., Johnson, J.D.: Sesame: the Los Alamos national laboratory equation of state database. Los Alamos National Laboratory, Los Alamos, NM, LA-UR-92-3407 (1992)
Jacobs, J.: Phys. Fluids A **5**, 2239 (1993)
Klein, R.I., McKee, C.F., Colella, P.: Astrophys. J. **420**, 213 (1994)
Klein, R.I., et al.: Astrophys. J. Suppl. Ser. **127**, 379–383 (2000)
Klein, R.I., et al.: Astrophys. J. **583**, 245 (2003)
Poludnenko, A., et al.: Astrophys. J. **576**, 832 (2002)
Poludnenko, A., et al.: Astrophys. J. **604**, 213 (2004)
Ranjan, D., Anderson, M., Oakley, J., Bonazza, R.: Phys. Rev. Lett. **94**, 184507 (2005)
Robey, H.F., et al.: Phys. Rev. Lett. **89**, 85001 (2002)
Rose, S.J.: J. Phys. B **25**, 1667 (1992)
Ryutov, D., Drake, R.P., Kane, J., Liang, E., Remington, B.A., Wood-Vasey, W.M.: Astrophys. J. **518**, 821 (1999)
Youngs, D.L.: In: Morton, K.W., Baines, M.J. (eds.) Numerical Methods for Fluid Mechanics. Academic Press, London (1982)
Youngs, D.L.: Physica D **12**, 32 (1984)